

Supporting Information for “Two-Dimensional III-Nitride Alloys: Electronic and Chemical Properties of Monolayer $\text{Ga}_{(1-x)}\text{Al}_x\text{N}$ ”

Yiqing Chen ¹, Ying Zhao ¹, Pengfei Ou ^{1,2*}, Jun Song ^{1*}

¹ Department of Mining and Materials Engineering, McGill University, 3610 University St, Montreal, QC H3A 0C5, Canada

² Department of Chemistry, Northwestern University, 2145 Sheridan Rd, Evanston, IL 60208, United States

Corresponding Author: * pengfei.ou@northwestern.edu (P. Ou); * jun.song2@mcgill.ca (J. Song).

S1. Optimized geometries of various $\text{Ga}_{(1-x)}\text{Al}_x\text{N}$ alloys

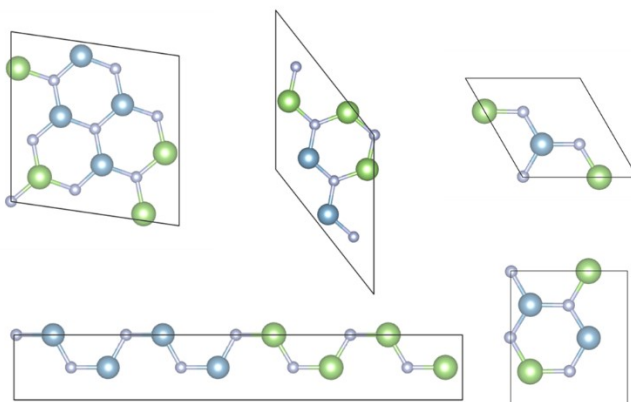


Fig. S1. Top views of optimized geometries of five representative $\text{Ga}_{(1-x)}\text{Al}_x\text{N}$ alloys generated by ATAT code. Ga, Al and N atoms are shown in green, blue and grey, respectively.

S2. Phonon calculations of 2D GaN, AlN and Ga_{0.5}Al_{0.5}N

Fig. S2 shows the calculated phonon dispersion curves of GaN, AlN and 2×2 Ga_{0.5}Al_{0.5}N, together with the corresponding phonon density of states (DOS). No imaginary frequencies are observed for all three structures, indicating their stabilities. Since 2×2 Ga_{0.5}Al_{0.5}N has the highest ΔH and is found to be stable. Therefore we believe it is reasonable to assume that other alloy configurations, with lower ΔH , would be stable. Besides, from the DOS plots, we can see that 2D GaN has a much larger band gap between phonon branches compared to that of 2D AlN, while 2×2 Ga_{0.5}Al_{0.5}N shows a band gap even smaller than 2D AlN. Such a trend is different from those for electronic band gaps in 2D Ga_(1-x)Al_xN, which have values between pristine GaN and AlN. As a result, changing the chemical composition could possibly affect the thermal and mechanical properties of 2D Ga_(1-x)Al_xN in a different manner.

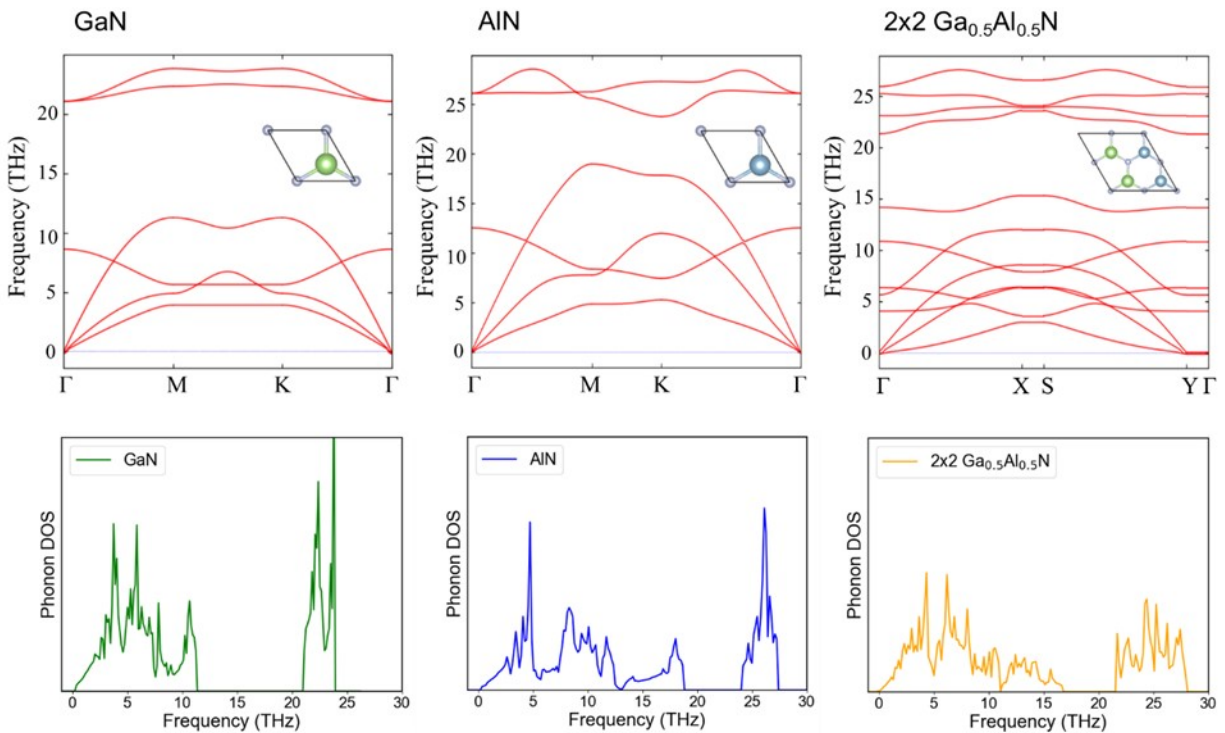


Fig. S2 Phonon dispersion curves and corresponding density of states (DOS) for 2D GaN, AlN and 2×2 Ga_{0.5}Al_{0.5}N, respectively. All results are calculated using PBE functionals. Corresponding atomic structures are shown in the insert figures in each plot.

S3. Vegard's law

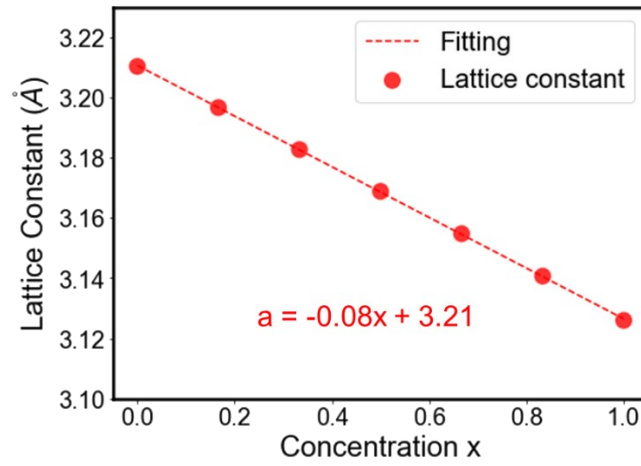


Fig. S3 Lattice constant (a , Å) of $\text{Ga}_{(1-x)}\text{Al}_x\text{N}$ random alloys as a function of concentration x .

S4. Band gap variation using 2×2 $\text{Ga}_{(1-x)}\text{Al}_x\text{N}$ ordered alloys

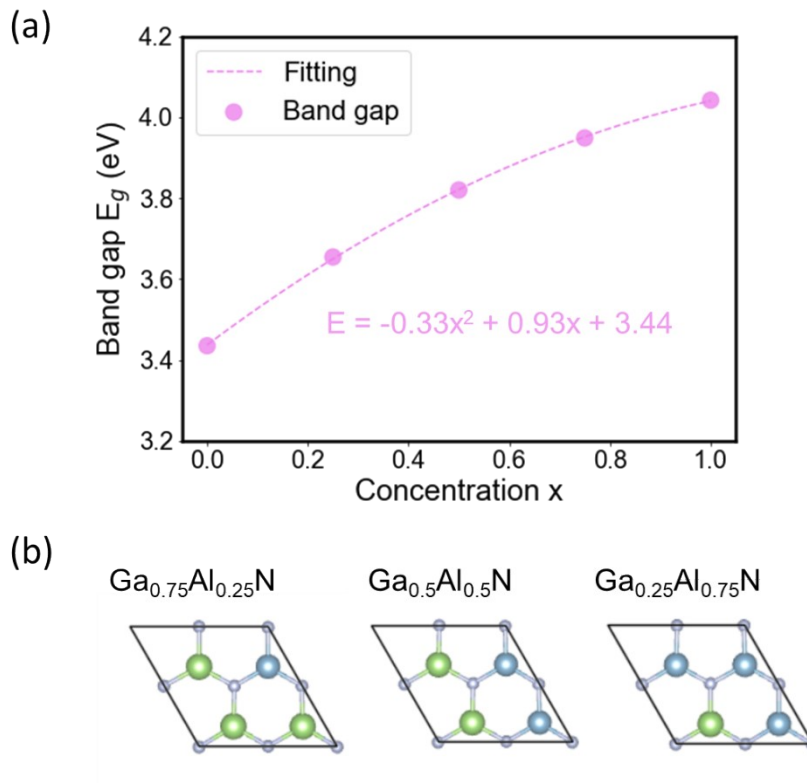


Fig. S4 (a) Band gap E_g of 2×2 $\text{Ga}_{(1-x)}\text{Al}_x\text{N}$ ordered alloys as a function of concentration x . (b) The top views of 2×2 $\text{Ga}_{(1-x)}\text{Al}_x\text{N}$ ordered alloys used for band gap calculations.

S5. Effect of functional choice on band gap calculations

We compared the results for band gaps calculated from HSE06 and PBE to investigate the effect of functional choice. This comparison is shown in Fig. S5. Our findings indicate that although the PBE functional underestimates the band gap of $\text{Ga}_{(1-x)}\text{Al}_x\text{N}$, it nevertheless yields a similar trend for band gap evolution with alloy concentrations, with a comparable bowing parameter b of -0.18 eV.

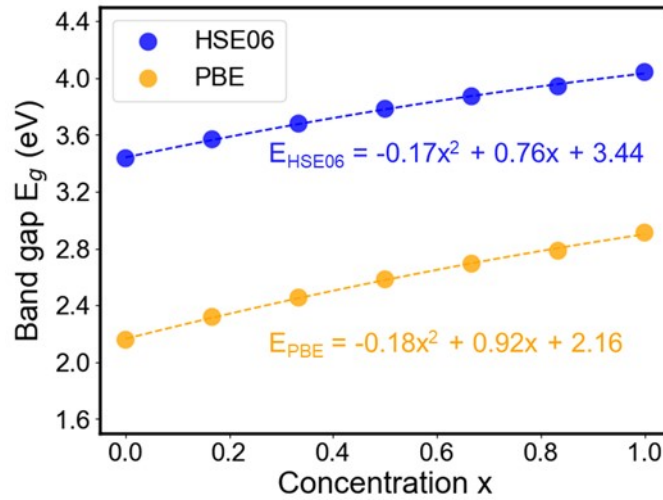


Fig. S5 Band gap E_g of $\text{Ga}_{(1-x)}\text{Al}_x\text{N}$ random alloys as a function of concentration x using HSE06 and PBE functionals, respectively.

S6. Mechanical stability of $\text{Ga}_{(1-x)}\text{Al}_x\text{N}$ alloys

We calculated the elastic constants of $\text{Ga}_{(1-x)}\text{Al}_x\text{N}$ random alloys at different concentrations using the PBE functional. The 2D III-nitride systems we considered exhibit a hexagonal structure and are 2D isotropic sheets, which only have two independent in-plane elastic constants, namely C_{11} and C_{12} (with $C_{66} = (C_{11} - C_{12})/2$) [1, 2]. The calculated values of C_{11} and C_{12} are summarized in Table S1 below. For the structure to be mechanically stable, it needs to satisfy the conditions of $C_{11} > 0$ and $C_{11} > C_{12}$ (so as $C_{66} > 0$). We can see that all the systems satisfy the conditions, and thus are expected to be mechanically stable.

Table S1 Calculated elastic constants of $\text{Ga}_{(1-x)}\text{Al}_x\text{N}$ random alloys at different concentration x .

Concentration x	C_{11} (N/m)	C_{12} (N/m)
0.00	136.15	58.98
0.17	127.68	50.37
0.33	133.83	56.55
0.50	140.74	63.06
0.67	147.86	70.44
0.83	143.91	65.41
1.00	145.68	66.44

S7. Optical properties of $\text{Ga}_{(1-x)}\text{Al}_x\text{N}$ alloys

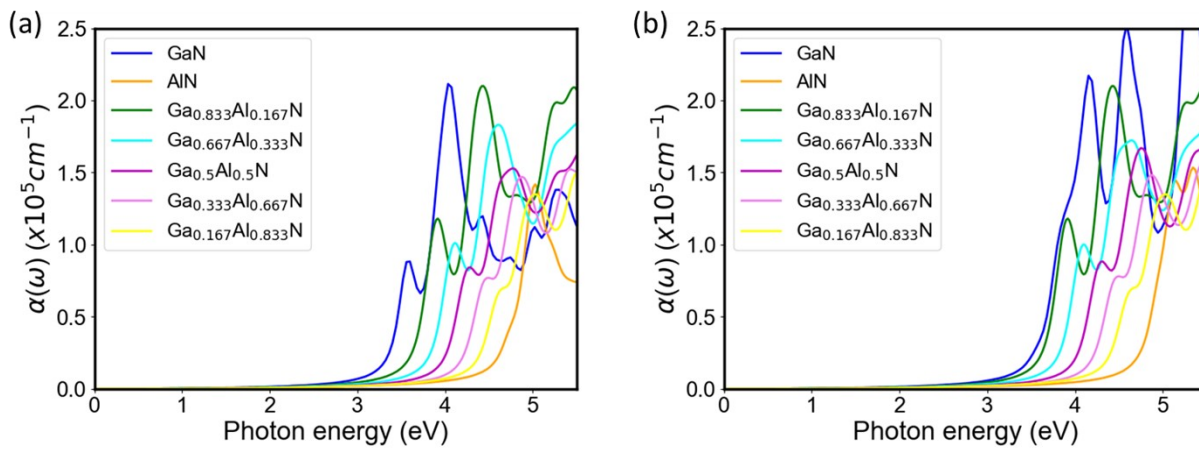


Fig. S6 Optical absorption of $\text{Ga}_{(1-x)}\text{Al}_x\text{N}$ random alloys along (a) x and (b) y directions at different concentrations calculated using HSE06 functionals.

S8. The ΔG_H of 2D $\text{Ga}_{(1-x)}\text{Al}_x\text{N}$ alloys as a function of concentrations

The ΔG_H value of $\text{Ga}_{(1-x)}\text{Al}_x\text{N}$ at each concentration corresponds to the most stable adsorption site on the alloy structure. It is found that increasing the Al concentration will monotonically increase the ΔG_H and thus decrease the HER activity.

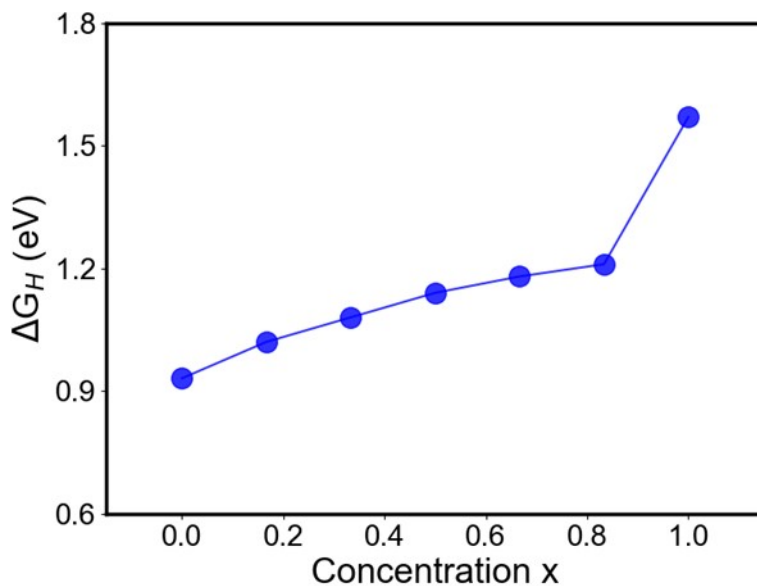


Fig. S7 Gibbs free energy of hydrogen adsorption G_H on $\text{Ga}_{(1-x)}\text{Al}_x\text{N}$ random alloy as a function of concentration x .

S9. Atomic configurations of reaction intermediates

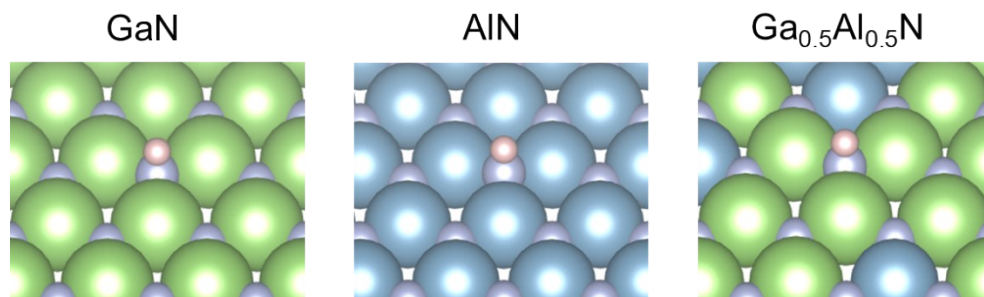


Fig. S8 Atomic configurations of hydrogen adsorption on GaN, AlN and Ga_{0.5}Al_{0.5}N, where Ga, Al, N and H atoms are shown in green, blue, grey and pink.

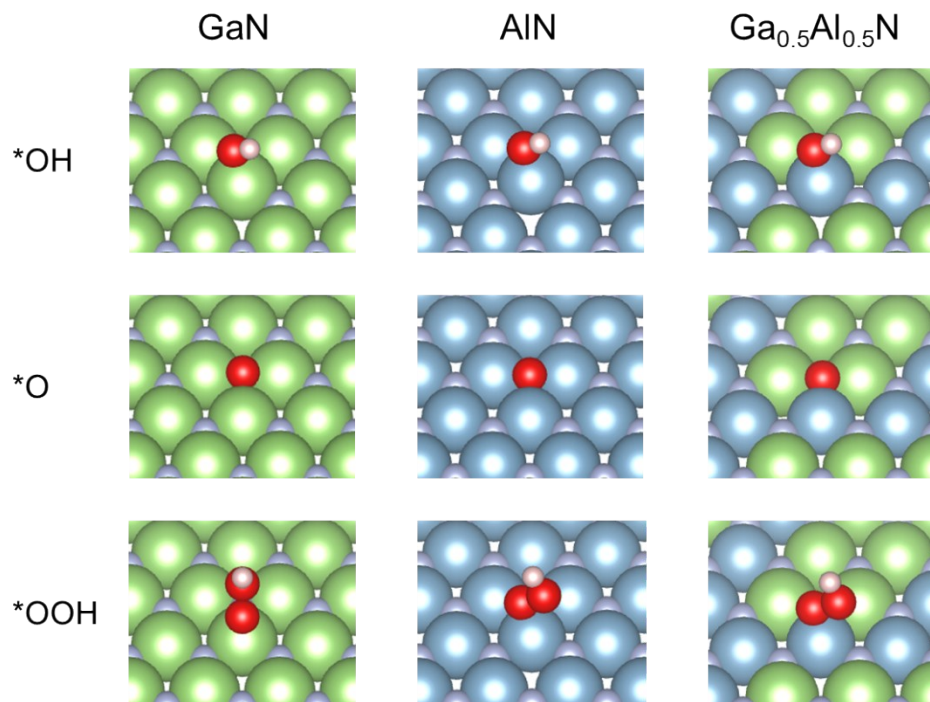


Fig. S9 Atomic configurations of each intermediate for OER on GaN, AlN and Ga_{0.5}Al_{0.5}N, where Ga, Al, N, O and H atoms are shown in green, blue, grey, red and pink.

Reference:

- [1] S.Y. Davydov, O.V. Posrednik, *Physics of the Solid State* 57 (2015) 837-843.
- [2] Q. Peng, C. Liang, W. Ji, S. De, *Applied Physics A* 113 (2013) 483-490.